Parasitol Res (2015) 114:3711–3719
DOI 10.1007/s00436-015-4600-2

ORIGINAL PAPER

Impact of gold nanoparticles on brain of mice infected with *Schistosoma mansoni*

Mohamed A. Dkhil[1,2] · **Amira A. Bauomy**[2,3] · **Marwa S.M. Diab**[4] · **Rizwan Wahab**[1] · **Denis Delic**[5] · **Saleh Al-Quraishy**[1,2]

Received: 5 June 2015 / Accepted: 18 June 2015 / Published online: 1 July 2015

Abstract Schistosomiasis is a condition characterized by high rates of morbidity and cognitive impairment. It afflicts many people in tropical and sub-tropical countries. Our study aimed to investigate the protective role of gold nanoparticles (GNPs) on the brain of mice infected with *Schistosoma mansoni*. Characterizations of GNPs were determined by using high-resolution transmission electron microscopy. Three doses of GNPs (0.25, 0.5, and 1.0 mg/kg body weight) were used to treat animals after *S. mansoni* infection. The infection induced impairments in histological picture as a result of schistosome infection resulting in a disturbance in the content of the brain neurotransmitters, norepinephrine (NE), and dopamine (DA). Also, the infection induced significant reduction in glutathione level; oppositely, the levels of nitric oxide and malondialdehyde were increased significantly. In addition, *S. mansoni* was able to disregulate the infected mice brain Cacnb4, Cabp4, Vdac3, Glrb, and Adam23 messenger RNA (mRNA). On the other hand, treatment of mice with GNPs could alleviate the histological impairments, the changes in the content of NE and DA, and the brain oxidative damage. Also, GNPs could regulate the gene expression due to *S. mansoni* infection. Generally, GNPs could decrease the neurooxidative stress and regulated the gene expression in the brain of infected mice. Consequently, our results revealed an anti-neuroschistosomal effect of GNPs in mice infected with *S. mansoni*.

Keywords *Schistosoma mansoni* · Gold nanoparticles · Brain · Neurotransmitters · Oxidative stress · Gene expression · Mice

✉ Saleh Al-Quraishy
guraishi@yahoo.com

[1] Department of Zoology, College of Science, King Saud University, P.O. Box 2455, Riyadh 11451, Saudi Arabia

[2] Department of Zoology and Entomology, Faculty of Science, Helwan University, Cairo, Egypt

[3] Department of Laboratory Sciences, College of Science & Arts, Al-Rass, Qassim University, Buraydah, Saudi Arabia

[4] Molecular Drug Evaluation Department, National Organization for Drug Control & Research (NODCAR), Giza, Egypt

[5] Boehringer-Ingelheim Pharma, Biberach, Germany

Introduction

Schistosomiasis is an important parasitic disease caused by trematode worms of the genus *Schistosoma*. This condition is characterized by high rates of morbidity, cognitive impairment, and incapacitation of affected individuals (Richter 2003). However, Schistosomiasis continues to spread in many parts of the world, especially due to lack of sanitation and irrigation projects (Steinmann et al. 2006). It is estimated that, each year, schistosomiasis afflicts up to 600 million people in 74 tropical and sub-tropical countries, predominantly in the developing world (El Ridi et al. 2014). Among the five different schistosome species, *Schistosoma mansoni* is the most abundant one in Egypt (Helmy et al. 2009).

Surprisingly, *S. mansoni* eggs and granulomas were identified in the central nervous system of symptomatic animals (Lambertucci et al. 2014). Central nervous system involvement can occur during acute primary infections (Chitsulo et al. 2000; Amaral et al. 2006). Neurological complications generally occur during chronic hepatointestinal schistosomiasis (Lambertucci 2010). Most pathology in schistosome-infected animals is attributed to the host's reaction to the eggs which is maximal by the eight week of infection.

In spite of remarkable chemotherapeutic progress and the existence of highly effective molecules such as the acylated quinoline–pyrazine praziquantel (PZQ), there is a spreading of schistosomiasis into new areas. It is generally agreed that chemotherapy, although the mainstay of current schistosomiasis control programs, does have some limitations. In addition, there is increasing concern about parasite resistance development (McManus and Loukas 2008).

Nanotechnology holds promise for medication and nutrition, because materials at the nanometer dimension exhibit novel properties different from those of both isolated atoms and bulk material.

Gold and silver nanoparticles have received special attention because they have found potential application in many fields of chemistry, physics, and biology because they possess an excellent biocompatibility and low toxicity and also because of their unique optical, electrical, and photothermal properties (Perez 2010; Isaac et al. 2013).

Recent interest in using gold nanoparticles (GNPs) in medicine has altered the methods of diagnosis and treatment (Chen et al. 2008; Peng et al. 2012). However, gold has a long history of use in the western world as nervine, a substance that could revitalize people suffering from nervous conditions. In addition, in the sixteenth century, it was recommended for the treatment of epilepsy (Richards et al. 2002).

GNPs have attracted great attention due to their unique electronic, optical, thermal, chemical, and biological properties and their potential catalytic applications in various fields such as biology, medicine, physics, chemistry, material science, and other interdisciplinary fields (Panyala et al. 2009). Although physicochemical properties of nanoparticles are well studied, their biological properties largely remain unexplored (Saritha et al. 2014). So, the aim of this study is to investigate the anti-schistosomal effect of GNPs on the neurotoxicity induced by *S. mansoni* in mice.

Materials and methods

Animals

Seventy-two male Swiss albino mice were bred under specified pathogen-free conditions and fed a standard diet and water ad libitum. Mice ages were 9 to 11 weeks and were approved by state authorities and followed Egyptian rules for animal protection.

Gold nanoparticles

GNPs have been prepared by chemical reduction method as reported by Turkevich et al. (1951). A solution of $HAuCl_4$ has been used as Au^{3+} ion precursor, while sodium citrate has been used as both of mild reducing and stabilizing agent. The color of the solution slowly turned into faint pink color, indicating the reduction of the Au^{3+} ions to Au nanoparticles.

Characterization

Size and morphology of GNPs were done by using transmission electron microscopy (TEM) equipped with high-resolution transmission electron microscope (HR-TEM). Samples for TEM were prepared using the colloidal solution of nanoparticles. The colloidal sample solution was sonicated for 10 min in a bath sonicator before the observation and dipped in carbon-coated copper grid (400 mesh) and dried at room temperature for the morphological analysis. A TEM picture was taken by a JOEL JEM 2000 EX 200 microscope at 200 kV.

Infection

S. mansoni cercariae were obtained from Schistosome Biological Supply Center at Theodor Bilharz Research Institute, Imbaba, Giza, Egypt. Mice were exposed to 100± 10*S. mansoni* cercariae per mouse by subcutaneous injection method modified by Oliver and Stirewalt (1952).

Experimental design

Animals were divided into six groups of 12 mice per group. Group I served as a control (noninfected control group). Each mouse of this group received 100 μl saline via intrapretonial injection (i.p.) for 10 days. Groups II, III, IV, V, and VI were infected with 100±10*S. mansoni* cercariae (Oliver and Stirewalt 1952). On day 46 postinfection (p.i.) with *S. mansoni*, the animals of groups III, IV, and V were intraperitonially injected with 100 μl of 0.25, 0.5, and 1.0 mg/kg GNPs, respectively, twice per week (on days 46 and day 49 p.i.). Finally, infected animals of group VI were orally administered 100 μl of PZQ (600 mg/kg body weight) on day 46 p.i. at an interval of 24 h for 2 days.

Brain tissue preparation

The animals of all groups were cervically decapitated, on day 56 p.i. with *S. mansoni*. Brains were rapidly excised from the skulls, blotted, and chilled. Brain tissue was divided into two halves. The first brain half of six mice were used for neurotransmitter estimation, and the second brain half of six mice were investigated for biochemical studies. The brain tissues were weighed, wrapped in plastic films, and quickly stored at −80 °C until used.

For investigating the brain histology, six half brains were fixed in 10 % neutral buffered formalin and embedded in paraffin, and 5-μm sections were stained with hematoxylin

and eosin. For the gene expression analysis, the six half brains were stored in RNAlater (Sigma-Aldrich).

Estimation of neurotransmitter contents

The brain norepinephrine (NE) and dopamine (DA) contents were estimated according to the method of Ciarlone (1978). For NE, flourimeter excitation was adjusted to 300 nm and emission at 480 nm. For DA, the excitation was at 320 nm and emission at 375 nm.

Biochemical studies

Brain tissues were homogenized in ice-cold medium containing 50 mM Tris–HCl and 300 mM sucrose, pH 7.4 (Tsakiris et al. 2004). This homogenate was used for biochemical determinations.

Glutathione

Glutathione (GSH) level in the brain was determined by the method of Ellman (1959). The method based on the reduction of Ellman's reagent with GSH to produce a yellow compound; the reduced chromogen directly proportional to GSH concentration and its absorbance can be measured at 405 nm.

Nitric oxide

Nitric oxide (NO) level was determined according to the method of Green et al. (1982) where, in an acid medium and in the presence of nitrite, the formed nitrous acid diazotize sulfanilamide is coupled with *N*-(1-naphthyl)ethylenediamine. The resulting azo dye has a bright reddish-purple color which can be measured at 540 nm.

Malondialdehyde levels

Malondialdehyde (MDA) level was determined according to the method of Ohkawa et al. (1979) by using 1 ml of trichloroacetic acid 10 % and 1 ml of thiobarbituric acid 0.67 % and was then heated in a boiling water bath for 30 min. Thiobarbituric acid-reactive substances were determined by the absorbance at 535 nm.

Quantitative real-time PCR

Total RNA was isolated with TRIzol (Sigma-Aldrich). Quality and integrity of RNA were determined using the Agilent RNA 6000 Nano Kit on the Agilent 2100 Bioanalyzer (Agilent Technologies). RNA was quantified by measuring A_{260nm} on the ND-1000 Spectrophotometer (NanoDrop Technologies) (Delic et al. 2010). Template complementary DNA (cDNA) was prepared using High Capacity cDNA Reverse Transcription Kit (Life Technologies, Darmstadt, Germany) according to the manufacturer's instructions. Quantitative real-time PCR (qRT-PCR) was performed using the ABI Prism 7900HT Sequence Detection System (Applied Biosystems, Darmstadt, Germany) with TaqMan Gene Expression Master Mix from Life Technologies (Darmstadt, Germany). TaqMan assays (Life Technologies, Darmstadt, Germany) used in the experiment are summarized in Table 1. For quantification, messenger RNA (mRNA) levels were normalized to those of GAPDH. The threshold cycle (C_T) value is the cycle number, selected from the logarithmic phase of the PCR curve, in which an increase in fluorescence above background can be detected. ΔC_T is determined by subtracting the C_T of GAPDH from the C_T of the target. The fold change of mRNA expression was determined using the $2^{-\Delta\Delta CT}$ method (Livak and Schmittgen 2001).

Statistical analysis

The obtained data were presented as means±standard error. One-way ANOVA was carried out, and the statistical comparisons among the groups were performed with Duncan's test using a statistical package program (SPSS version 17.0). $P \leq 0.05$ was considered as significant for all statistical analysis in this study.

Results

The structural morphology and crystalline character of GNPs were examined via transmission electron microscopy (TEM) equipped with high-resolution transmission electron microscopy (HR-TEM). The obtained images show the corresponding TEM results, which are shown in Fig. 1. The low-magnified image shows that the GNPs are spherical in shape within the range of 10–15 nm in diameter. From the observation, it is depicted that all the GNPs are in definite spherical shape with rough surface and free from agglomeration behavior. Another obtained image represents the high-resolution TEM (HR-TEM) image of GNPs (Fig. 1a), which shows that the lattice difference fringes between two adjacent planes are about 0.235 nm. The obtained lattice difference clearly corresponds to the lattice constant of face-centered cubic (FCC) of GNPs and is analogous with the previously reported information (Balmes et al. 2006; Wang et al. 2009). The crystal lattice fringes of HR-TEM observation (Fig. 1b) again show a confirmation of good crystalline nature of synthesized GNPs, and it is consistent with the low-magnified image of GNPs (Balmes et al. 2006; Wang et al. 2009).

Our microscopic findings revealed marked histopathological impairments, neuronal loss, vacuolated cytoplasm, nuclear hyperchromasia, marked dilated congested blood capillaries accompanied with vessel wall edema, and presence of

Table 1 Primer assays used for qRT-PCR analysis

Gene	TaqMan assay name	PCR product size (bp)
Calcium channel, voltage-dependent, beta 4 subunit (Cacnb4)	Mm00521623_m1	78
Calcium-binding protein 4 (Cabp4)	Mm00600215_m1	66
Voltage-dependent anion channel 3 (Vdac3)	Mm04213589_g1	77
Glycine receptor, beta subunit (Glrb)	Mm00439140_m1	63
A disintegrin and metallopeptidase domain 23 (Adam23)	Mm00478606_m1	59
Glyceraldehyde 3-phosphate dehydrogenase (GAPDH)	Mm99999915_g1	107

extravasated red blood cells in brain tissue of schistosome-infected mice as compared to noninfected control group (Fig. 2). On the other hand, the treatment of the schistosome-infected mice with three different doses of GNPs (0.25, 0.5, and 1.0 mg/kg) recorded histological alleviations (Fig. 2).

The schistosome-infected mice showed a significant reduction in brain NE content as compared to noninfected control group (Table 2). The treatment of schistosome-infected mice with GNPs at three different doses (0.25, 0.5, and 1.0 mg/kg body weight) induced a significant increase ($P \leq 0.05$) in brain NE content as compared to both noninfected control and infected groups. In the same line, the treatment with PZQ cleared a significant increase in the NE content. Also, the *S. mansoni* infection significantly decreased brain DA content in mice, as compared to control group. A significant decrease ($P \leq 0.05$) was noticed in DA content in schistosome-infected mice treated with 0.25 and 0.5 mg/kg GNPs and+PZQ as compared to noninfected control group. On contrary, the administration of the higher dose of GNPs (1.0 mg/kg) resulted in a significant elevation in DA content versus control group. The content of brain DA showed a significant increase in all treated groups as compared to schistosome-infected group (Table 2).

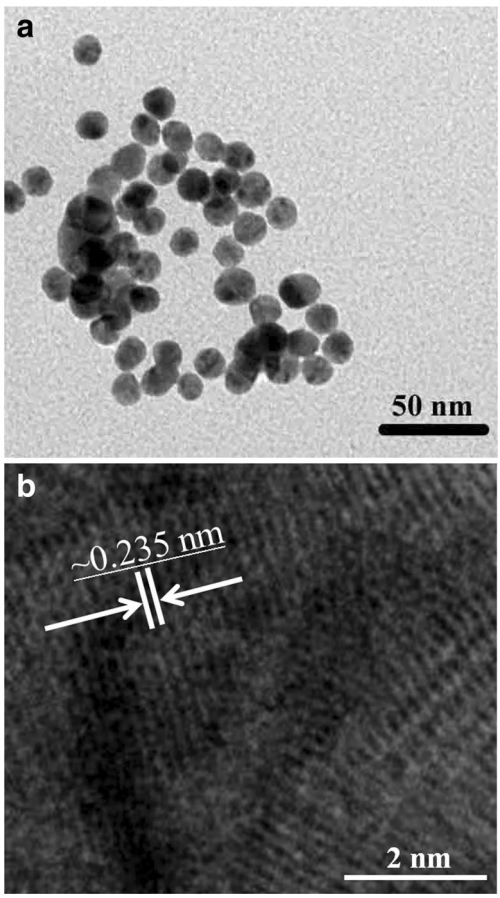

Fig. 1 Typical TEM and their corresponding HR-TEM images of synthesized GNPs: **a** Low-magnification image of spherical GNPs (~10–15 nm) and **b** HR-TEM image of difference between two lattice fringes, which is ~0.235 nm

The schistosomiasis induced a significant reduction in brain GSH level as shown in Fig. 3. Likewise, treatment with GNPs (0.25, 0.5, and 1.0 mg/kg) and+PZQ significantly reduced GSH level versus noninfected control group. On the other hand, a significant increase was found in GSH level as a result of GNP injection (0.25 mg/kg) to the infected mice as compared to schistosome-infected mice, while a nonsignificant increase was recorded in brain GSH level due to injection of both doses of GNPs (+0.5 and +1 mg/kg) and+PZQ to the infected mice.

A significant elevation was recorded in both levels of brain NO and MDA (Figs. 4 and 5, respectively) of schistosome-infected mice as compared to the noninfected group. Oppositely, treatment with 0.25, 0.50, and 1.0 mg GNPs/kg b. wt and+PZQ to schistosome-infected mice influenced a significant decrease in NO level, while a nonsignificant change was obtained in brain MDA level as a result of PZQ treatment versus infected group.

S. mansoni was able to induce a significant upregulation in Adam23, Glrb, Vdac3, and Cacnb4 mRNA expressions; on contrary, Cabp4 mRNA expression showed a significant downregulation as compared to noninfected group (Fig. 6). Only, Vdac3 and Cabp4 mRNA expressions were significantly increased in the brain of mice infected with *S. mansoni*, after the administration of GNPs at a dose of 0.25 and 1.0 mg/kg, respectively. The expressions of Adam23, Grlb,

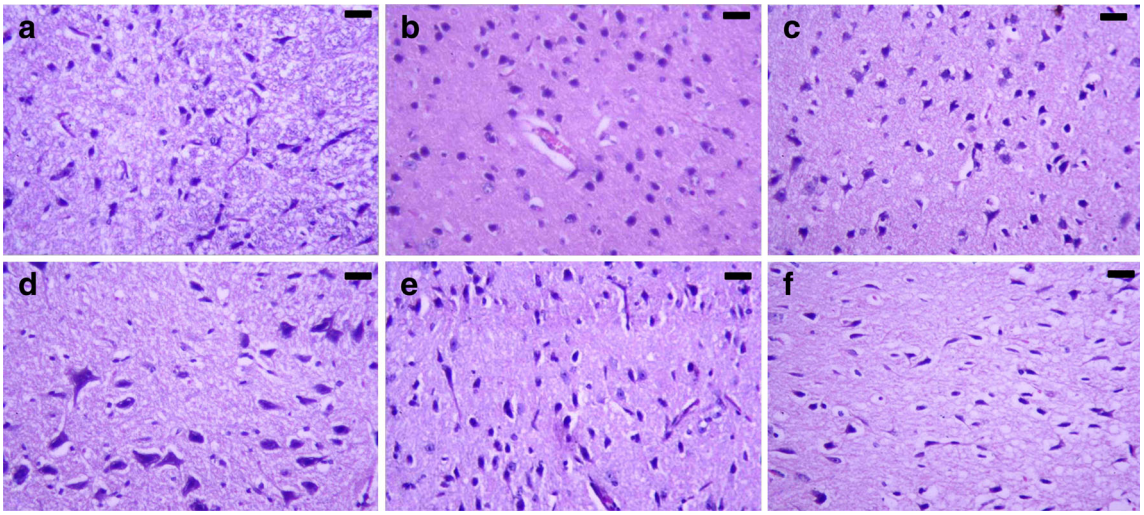

Fig. 2 GNPs induced changes in the histological architecture of mice brain infected with *S. mansoni* on day 46 p.i. **a** Noninfected brain with normal architecture, **b** infected brain tissue with distorted brain parenchyma and pericellular edema, and **c**–**f** infected-treated mice with 0.25, 0.5, and 1.0 mg/kg GNPs, respectively. Brain appeared with fewer lesions, and tissue damage appears to be minimized. Sections are stained with hematoxylin and eosin. *Bar*=25 μm

and Cacnb4 mRNA were downregulated as a result of GNP treatment at different doses. Meanwhile, Vdac3 mRNA expression cleared a significant reduction as GNP treatment at 0.5 and 1.0 mg/kg.

Discussion

Since, schistosomiasis is an endemic disease which, on a global scale, 779 million people are at risk of contracting the disease (Coeli et al. 2013). Therefore, research trials have been carried out to study the new approach to the experimental treatment for schistosomiasis. Somehow, the extensive use of PZQ develops *Schistosoma* sp. resistant to treatment (Fallon and Doenhoff 1994). Since there are few other options regarding the treatment for schistosomiasis (Doenhoff et al. 2009), in particular for *S. mansoni*, it is necessary to search for alternative drugs.

In the present study, the schistosomiasis which resulted in a significant reduction in both brain NE and DA contents was recorded in schistosome-infected mice as compared to noninfected mice. Our results are in agreement with Abdel Ghafar et al. (1996) and Bauomy et al. (2013).

The treatment of schistosome-infected mice with different doses of GNPs (0.25, 0.5, and 1.0 mg/kg) caused a significant alleviation in content of NE and DA. Ancient cultures in Egypt, India, and China used gold to treat some diseases (Chen et al. 2008). Moreover, gold complexes with different organic drugs have been tested as ligands against malaria, trypanosomiasis, and leishmaniasis (Navarro et al. 2007). It is worth mentioning that the GNPs have also been used for the diagnosis of Alzheimer's disease and activated microglia (Nunes et al. 2012).

The oxidative damage in stress could contribute to the degenerative diseases of aging, including brain dysfunction (Liu et al. 1996). The early-onset decline in learning and memory is associated with a very significant increase in two parameters

Table 2 Effect of gold nanoparticles on brain neurotransmitters norepinephrine (NE) and dopamine (DA) on *S. mansoni*-infected mice

Group	Norepinephrine (μg/g tissue)	Dopamine (μg/g tissue)
Noninfected	290.2±2.93	877.8±2.67
Infected (-GNP)	263.3±2.80*	778.6±2.08*
Infected (+0.25 mg/kg GNP)	339.0±2.59*,**	842.8±2.85*,**
Infected (+0.5 mg/kg GNP)	331.5±2.62*,**	838.1±2.50*,**
Infected (+1 mg/kg GNP)	324.0±2.44*,**	1011.2±4.58*,**
Infected (+PZQ)	330.6±2.08*,**	798.4±3.54*,**

Values are means±SEM

*Significant against noninfected (-GNPs) group at $P \leq 0.05$; **significant against infected (-GNPs) group at $P \leq 0.05$

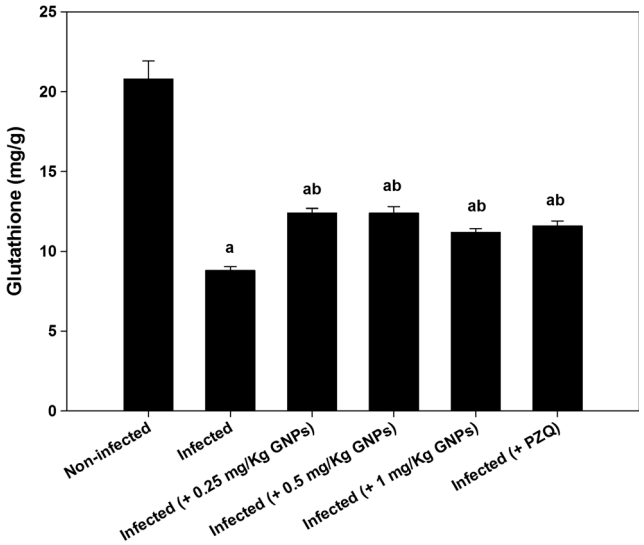

Fig. 3 Level of reduced glutathione (GSH) in infected mice brain tissue with *S. mansoni* and treated with different doses of gold nanoparticles. Values are means±SEM. Significant against noninfected (-GNPs) group at $P \leq 0.05$ (*a*). Significant against infected (-GNPs) group at $P \leq 0.05$ (*b*)

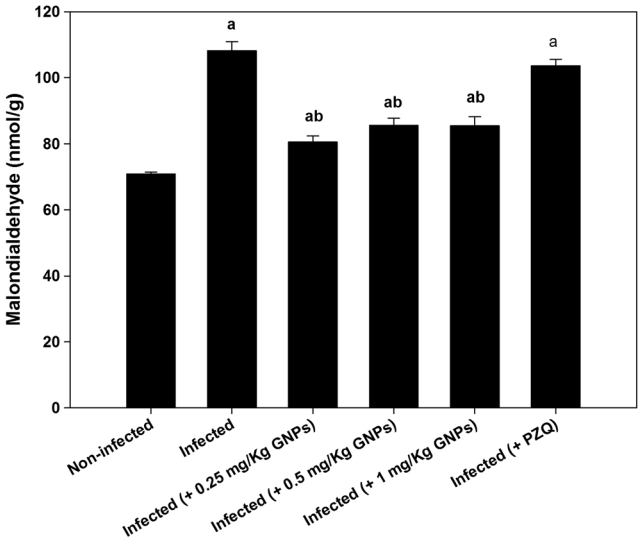

Fig. 5 Gold nanoparticles ameliorated MDA level in brain homogenate of *S. mansoni*-infected mice. Values are means±SEM. Significant against noninfected (-GNPs) group at $P \leq 0.05$ (*a*). Significant against infected (-GNPs) group at $P \leq 0.05$ (*b*)

of oxidative stress in the brain, levels of lipid peroxidation and of protein oxidation (Liu et al. 2003).

However, schistosomiasis induced a significant reduction in brain GSH level and a significant elevation in both levels of NO and MDA. These results are in agreement with many studies (de Oliveira et al. 2013; Diab et al. 2013; Bauomy 2014; Bauomy et al. 2014; Dkhil 2014). Also, de Oliveira et al. (2013) cleared that *S. mansoni* had altered nonenzymatic antioxidant status in the brain. In addition, Bauomy (2014) reported that schistosomiasis induced brain oxidative stress as evidenced by the decrease of GSH level, total antioxidant capacity, and the activity of catalase significantly, while a significant elevation in the levels of nitrite/nitrate and MDA. Furthermore, in different mice organs, *S. mansoni* infection decreased GSH level, the activities of catalase, and superoxide dismutase significantly and, on contrary, increased NO and MDA levels significantly (Diab et al. 2013; Bauomy et al. 2014; Dkhil 2014).

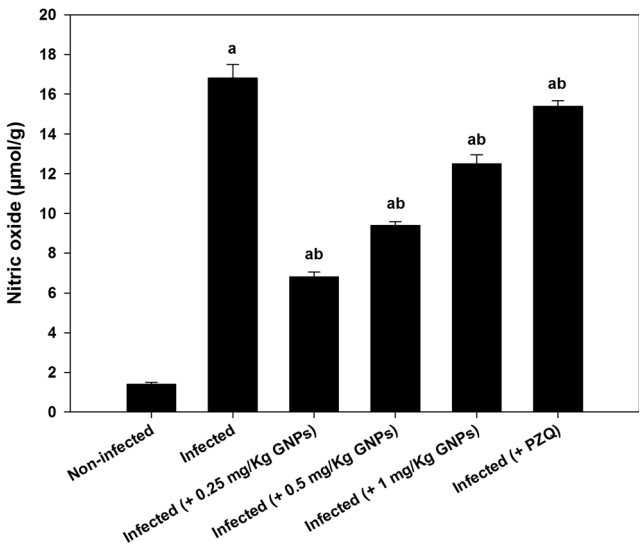

Fig. 4 Changes in brain NO level in the brain of *S. mansoni*-infected mice and treated with nanogold particles (GNPs) at three different doses. Values are means±SEM. Significant against noninfected (-GNPs) group at $P \leq 0.05$ (*a*). Significant against infected (-GNPs) group at $P \leq 0.05$ (*b*)

Moreover, GNP injection at different doses to schistosome-infected mice resulted in a significant increase in GSH level and a significant decrease in NO and MDA levels as compared to schistosome-infected mice. The mechanisms of action of gold drugs are poorly understood (Best and Sadler 1996). Typically, after systemic administration, the nanoparticles are small enough to penetrate very small capillaries throughout the body, and therefore, they could offer the most effective approach to target certain tissues (Braydich-Stolle et al. 2005), such as brain, and can affect the physiology of any cell in an animal body (Brooking et al. 2001).

However, our histological findings emphasized that the GNP treatment to schistosome-infected mice resulted in alleviation of the brain histological impairments. The present records go hand in hand with those of Lasagna-Reeves et al. (2010), where the authors deduced a clear increase on GNP accumulation at increasing doses supporting the possibility to use nanoparticles to target the brain without producing detectable toxicity. This is important for the utilization of GNPs for potential treatment and diagnosis of neurodegenerative disorders. The pharmacokinetic, bioavailability, bioaccumulation, clearance, and toxicity of nanoparticles are likely dependent of the particle composition, size, and surface characteristics.

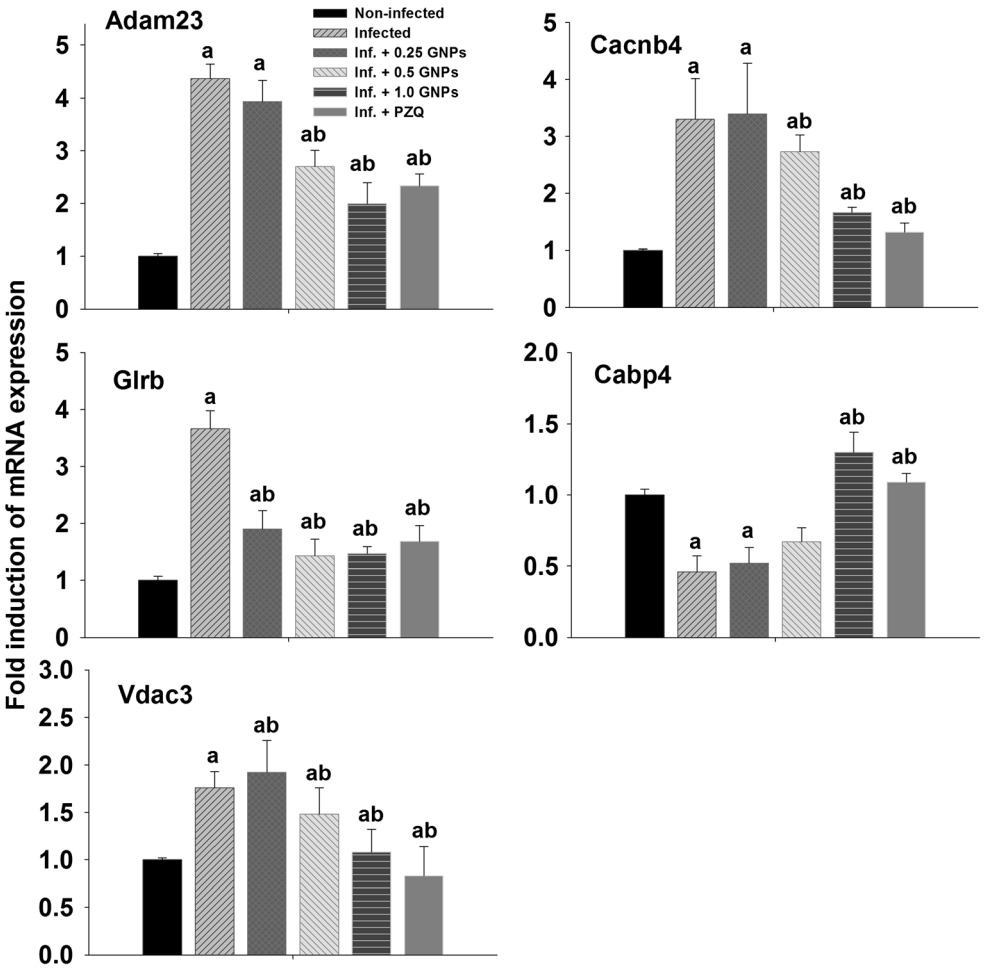

Fig. 6 Gold nanoparticles induced changes in gene expression of mice brain infected with *S. mansoni*. Expression of Adam23, Glrb, Vdac3, Cacnb4, and Cabp4 in brain tissues was analyzed by quantitative RT-PCR in noninfected mice and *S. mansoni*-infected mice on day 59 p.i. with and without GNP treatment. Relative expression is given as fold increase in comparison with noninfected control mice. Values are means± SD. Significant against noninfected (-GNPs) group at $P \leq 0.05$ (*a*). Significant against infected (-GNPs) group at $P \leq 0.05$ (*b*)

Since, schistosomiasis increased brain Adam23 gene expression. Sagane et al. (1999) and Mitchell et al. (2001) reported that disruption of the mouse Adam23 induced neurological defects, ataxia, and premature death, indicating that this protein is important for normal brain development. On the other hand, injection of GNPs recorded a significant downregulation in brain Adam23 gene.

Glrb gene encodes the inhibitory human glycine receptor β subunit (Lee et al. 2013). Inhibitory glycinergic synapses are located predominantly in the spinal cord and brainstem (Chalphin and Saha 2010), and disruptions to their function increase the general level of excitability of motor neurons, thus accounting for neonatal hypertonia. Glrb is one of the adult walking behaviors which recorded high expression in the malarial brain (Desruisseaux et al. 2010). These results are in agreement with our records in which schistosomiasis induced a significant overexpression in brain Glrb gene. On contrary, gene amelioration resulted in GNP treatment. In the present result, Vdac3 gene recorded a significant overexpression as a result of schistosomiasis. Cízková et al. (2008) reported that Vdac3 is a mitochondrial gene that is regulated in the malaria brain whose dysfunction is associated with neurological disorders. Our results pointed that GNP and PZQ treatment to schistosome-infected mice induced downregulation in Vdac3 brain gene.

Cacnb4 gene mutations encoding voltage-gated calcium channels (VGCCs) induce diverse neuronal pathologies, such as epilepsy, ataxia, autism, and migraine (Bidaud et al. 2006). It is known that neuroschistosomiasis induced ataxia, headache as a common manifestation (Ferrari 2004).

In the present work, Cacnb4 gene recorded a significant upregulation, while Cabp4 gene showed a significant downregulation as a result of neuroschistosomiasis. It was reported that calcium current through VGCCs controls gene expression (Tadmouri et al. 2012). Barnes and Kelly (2002) deduced that calcium influx through calcium channels triggers neurotransmitter release where increase the release of the neurotransmitters by exocytosis, and this may explain reduced contents of DA and NE in our investigations. VGCCs mediate the influx of calcium ions into the cell upon membrane polarization which control multiple neuronal functions including excitability, synaptic transmission, and activity-dependent gene regulation (Catterall and Few 2008). Cabp4 may be an important regulator of calcium influx and transmitter release in synaptic

terminals (Haeseleer et al. 2004). Cabp4 interacts with calmodulin-binding sequences in VGCC which weakly inhibits calcium-dependent inactivation.

Comparing results of treatment of GNPs with those of praziquantel, we can say that treatment with GNPs may be a promising way against neuroschistosomiasis, but further studies are required to know the mechanism of GNP action and the best safe dose for the treatment.

Collectively, GNP treatment for neuroschistosomiasis improved the histopathological changes resulted in the brain of schistosome-infected mice, as well as ameliorated the disturbances in brain neurotransmitters. In addition, GNPs at all investigated doses decreased the neurooxidative stress and regulated the gene expression in the brain of infected mice. Consequently, our results revealed an anti-neuroschistosomal effect in mice infected with *S. mansoni*.

Acknowledgments The authors extend appreciations to the Deanship of Scientific Research at King Saud University for funding the work through the research group project number PRG-1436-02.

References

Abdel Ghafar AE, Elkowrany SE, Salem SA, Menaisy AA, Fadel WA, Awara WM (1996) Effect of some parasitic infection on neurotransmitters in the brain of experimentally infected mice before and after treatment. J Egypt Soc Parasitol 26(2):497–508

Amaral RS, Tauil P, Lima DD, Engels D (2006) An analysis of the impact of the schistosomiasis control programme in Brazil. Mem Inst Oswaldo Cruz 101:79–85

Balmes O, Malm J, Pettersson N, Karlsson G, Bovin J (2006) Imaging atomic structure in metal nanoparticles using high-resolution cryo-TEM. Microsc Microanal 12(02):145–150

Barnes S, Kelly MEM (2002) Calcium channels at the photoreceptor synapse. Adv Exp Med Biol 514:465–476

Bauomy AA (2014) The potential role of *Morus alba* leaves extract on the brain of mice infected with *Schistosoma mansoni*. CNS Neurol Disord Drug Targets 13:1513–1519

Bauomy A, Diab M, Abdel Moneim AE, Dkhil MA, Al-Quraishy S (2013) Neuronal activities of berberine in Schistosoma mansoni infected mice. Afr J Pharm Pharmacol 7:368–374

Bauomy AA, Dkhil MA, Diab MSM, Amer OSO, Zrieq RM, Al-Quraishy S (2014) Response of spleen and jejunum of mice infected with *Schistosoma mansoni* to mulberry treatment. Pakistan J Zool 46:753–761

Best SL, Sadler P (1996) Gold drugs: mechanism of action and toxicity. Gold Bull 29(3):87–93

Bidaud I, Mezghrani A, Swayne LA, Monteil A, Lory P (2006) Voltage-gated calcium channels in genetic diseases. Biochim Biophys Acta 1763:1169–1174

Braydich-Stolle L, Hussain S, Schlager JJ, Hofmann MC (2005) In vitro cytotoxicity of nanoparticles in mammalian germline stem cells. Toxicol Sci 88:412–419

Brooking J, Davis SS, Illum L (2001) Transport of nanoparticles across the rat nasal mucosa. J Drug Target 9:267–279

Catterall WA, Few AP (2008) Calcium channel regulation and presynaptic plasticity. Neuron 59:882–901

Chalphin AV, Saha MS (2010) The specification of glycinergic neurons and the role of glycinergic transmission in development. Front Mol Neurosci 3:11

Chen PC, Mwakwari SC, Oyelere AK (2008) Gold nanoparticles: from nanomedicine to nanosensing. Nanotechnol Sci Appl 2:45–66

Chitsulo L, Engels D, Montresor A, Savioli L (2000) The global status of schistosomiasis and its control. Acta Trop 77:41–51

Ciarlone AE (1978) Further modification of a fluorometric method for analyzing brain amines. Microchem J 23:9–12

Cízková A, Stránecký V, Mayr JA, Tesarová M, Havlícková V, Paul J, Ivánek R, Kuss AW, Hansíková H, Kaplanová V, Vrbacký M, Hartmannová H, Nosková L, Honzík T, Drahota Z, Magner M, Hejzlarová K, Sperl W, Zeman J, Houstek J, Kmoch S (2008) TMEM70 mutations cause isolated ATP synthase deficiency and neonatal mitochondrial encephalocardiomyopathy. Nat Genet 40: 1288–1290

Coeli R, Baba EH, Araujo N, Coelho PMZ, Oliveira G (2013) Praziquantel treatment decreases *Schistosoma mansoni* genetic diversity in experimental infections. PLoS Negl Trop Dis 7(12), e2596

de Oliveira RB, Senger MR, Vasques LM et al (2013) *Schistosoma mansoni* infection causes oxidative stress and alters receptor for advanced glycation endproduct (RAGE) and tau levels in multiple organs in mice. Int J Parasitol 43(5):371–379

Delic D, Grosser C, Dkhil M, Al-Quraishy S, Wunderlich F (2010) Testosterone-induced upregulation of miRNAs in the female mouse liver. Steroids 75:998–1004

Desruisseaux MS, Iacobas DA, Iacobas S, Mukherjee S, Weiss LM, Tanowitz HB, Spray DC (2010) Alterations in the brain transcriptome in *Plasmodium berghei* ANKA infected mice. J Neuroparasitol 1:1–11

Diab MSM, Bauomy AA, Dkhil MA, Amer OSO, Al-Quraishy S (2013) Role of *Morus alba* in ameliorating *Schistosoma mansoni*-induced renal and testicular injuries in mice. Pakistan J Zool 45:1367–1375

Dkhil MA (2014) Role of berberine in ameliorating Schistosoma mansoni-induced hepatic injury in mice. Biol Res 47(1):8

Doenhoff MJ, Hagan P, Cioli D, Southgate V, Pica-Mattoccia L, Botros S, Coles G, Tchuem Tchuenté LA, Mbaye A, Engels D (2009) Praziquantel: its use in control of schistosomiasis in sub-Saharan Africa and current research needs. Parasitology 136:1825–1835

El Ridi R, Tallima H, Dalton JP, Donnelly S (2014) Induction of protective immune responses against schistosomiasis using functionally active cysteine peptidases. Front Genet 8:119

Ellman GL (1959) Tissue sulfhydryl groups. Arch Biochem Biophys 82: 70–77

Fallon PG, Doenhoff MJ (1994) Drug-resistant schistosomiasis: resistance to praziquantel and oxamniquine induced in *Schistosoma mansoni* in mice is drug specific. Am J Trop Med Hyg 51:83–88

Ferrari TC (2004) Involvement of central nervous system in the schistosomiasis. Mem Inst Oswaldo Cruz 99:59–62

Green LC, Wagner DA, Glogowski J, Skipper PL, Wishnok JS, Tannenbaum SR (1982) Analysis of nitrate, nitrite, and [15N] nitrate in biological fluids. Anal Biochem 126:131–138

Haeseleer F, Imanishi Y, Maeda T, Possin DE, Maeda A, Lee A, Rieke F, Palczewski K (2004) Essential role of Ca^{2+}-binding protein 4, a Cav1.4 channel regulator, in photoreceptor synaptic function. Nat Neurosci 7(10):1079–1087

Helmy M, Mahmoud S, Fahmy Z (2009) *Schistosoma mansoni*: effect of dietary zinc supplement on egg granuloma in Swiss mice treated with praziquantel. Exp Parasitol 122:310–317

Isaac RSR, Sakthivel G, Murthy C (2013) Green synthesis of gold and silver nanoparticles using Averrhoa bilimbi fruit extract. J Nanotechnol 2013:6. doi:10.1155/2013/906592

Lambertucci JR (2010) Acute *schistosomiasis mansoni*: revisited and reconsidered. Mem Inst Oswaldo Cruz 105:422–435

Lambertucci JR, Fidelis TA, Pereira TA, Coelho PM, Araujo N, Souza MM, Filho BG, Pereira FE, Antunes CM (2014) Brain

schistosomiasis in mice experimentally infected with *Schistosoma mansoni*. Rev Soc Bras Med Trop 47(2):251–253

Lasagna-Reeves C, Gonzalez-Romero D, Barria MA, Olmedo I, Clos A, Sadagopa Ramanujam VM, Urayama A, Vergara L, Kogan MJ, Soto C (2010) Bioaccumulation and toxicity of gold nanoparticles after repeated administration in mice. Biochem Biophys Res Commun 393:649–655

Lee CG, Kwon MJ, Yu HJ, Nam SH, Lee J, Ki CS, Lee M (2013) Clinical features and genetic analysis of children with hyperekplexia in Korea. J Child Neurol 28:90–94

Liu J, Wang X, Shigenaga MK, Yeo HC, Mori A, Ames BN (1996) Immobilization stress causes oxidative damage to lipid, protein, and DNA in the brain of rats. T FASEB J 10:1532–1538

Liu R, Liu IY, Bi X, Thompson RF, Doctrow SR, Malfroy B, Baudry M (2003) Reversal of age-related learning deficits and brain oxidative stress in mice with superoxide dismutase catalase mimetics. PNAS 100:8526–8531

Livak KJ, Schmittgen TD (2001) Analysis of relative gene expression data using real-time quantitative PCR and the 2(-Delta Delta C(T)) Method. Methods 25:402–408

McManus DP, Loukas A (2008) Current status of vaccines for schistosomiasis. Clin Microbiol Rev 21:225–242

Mitchell KJ, Pinson KI, Kelly OG, Brennan J, Zupicich J, Scherz P, Leighton PA, Goodrich LV, Lu X, Avery BJ, Tate P, Dill K, Pangilinan E, Wakenight P, Tessier-Lavigne M, Skarnes WC (2001) Functional analysis of secreted and transmembrane proteins critical to mouse development. Nat Genet 28:241–249

Navarro M, Hernandez C, Colmenares I, Hernandez P, Fernandez M, Sierraalta A (2007) Synthesis and characterization of [Au(dppz)2] Cl3. DNA interaction studies and biological activity against Leishmania (L) mexicana. J Inorg Biochem 101:111–116

Nunes A, Al-Jama KT, Kostarelos K (2012) Therapeutics, imaging and toxicity of nanomaterials in the central nervous system. J Control Release 161:290–296

Ohkawa H, Ohishi N, Yagi K (1979) Assay for lipid peroxides in animal tissues by thiobarbituric acid reaction. Anal Biochem 95:351–358

Oliver L, Stirewalt MA (1952) An efficient method for the exposure of mice to cercaria of Schistosoma mansoni. J Parasitol 38:19–23

Panyala NR, Peña-Méndez EM, Havel J (2009) Gold and nano-gold in medicine: overview, toxicology and perspectives. J Appl Biomed 7: 75–91

Peng Y, Wu J, Wang J, Li W, Yu S (2012) Study and evaluation of Wondfo rapid diagnostic kit based on nano-gold immunochromatography assay for diagnosis of *Plasmodium falciparum*. Parasitol Res 110:1421–1425

Perez DP (ed) (2010) Nanotechnology and Nanomaterials "Silver nanoparticles" Chapter 13: biosynthesis and application of silver and gold nanoparticles "*Sadowski Z*". InTech

Richards DG, McMillin DL, Mein EA, Nelson CD (2002) Gold and its relationship to neurological/glandular conditions. Int J Neurosci 112:31–53

Richter J (2003) The impact of chemotherapy on morbidity due to schistosomiasis. Acta Trop 86:161–183

Sagane K, Yamazaki K, Mizui Y, Tanaka I (1999) Cloning and chromosomal mapping of mouse. ADAM11, ADAM22 and ADAM23. Gene 236:79–86

Saritha K, Saraswathi U, Singaravelu G, Revathi S, Jayanthi V (2014) Biological synthesis and characterization of gold nanoparticles using Lemna minor. Asian J Pharm Clin Res 7(2):165–167

Steinmann P, Keiser J, Bos R, Tanner M, Utzinger J (2006) Schistosomiasis and water resources development: systematic review, meta-analysis, and estimates of people at risk. Lancet Infect Dis 6(7):411–425

Tadmouri A, Kiyonaka S, Barbado M, Rousset M, Fablet K, Sawamura S, Bahembera E, Pernet-Gallay K, Arnoult C, Miki T, Sadoul K, Gory-Faure S, Lambrecht C, Lesage F, Akiyama S, Khochbin S, Baulande S, Janssens V, Andrieux A, Dolmetsch R, Ronjat M, Mori Y, De Waard M (2012) Cacnb4 directly couples electrical activity to gene expression, a process defective in juvenile epilepsy. EMBO J 31(18):3730–3744

Tsakiris S, Schulpis KH, Marinou K, Behrakis P (2004) Protective effect of l-cysteine and glutathione on the modulated suckling rat brain Na^+, K^+, -ATPase and Mg^{2+} -ATPase activities induced by the *in vitro* galactosaemia. Pharmacol Res 49:475–479

Turkevich J, Stevenson PC, Hiller J (1951) Discuss. Faraday Soc 11:55–75

Wang YQ, Liang WS, Geng CY (2009) Coalescence behavior of gold nanoparticles. Nanoscale Res Lett 4(7):684–688